Supporting Information

Tuning the Spin-Crossover properties of [Fe_2] Metal-Organic Cages

*Laia Navarro[1], Arnau Garcia-Duran[1] and Jordi Cirera[1]**

[1] Departament de Química Inorgànica i Orgànica and Institut de Recerca de Química Teòrica i Computacional, Universitat de Barcelona,
Diagonal 645, 08028, Barcelona, Spain

e-mail: jordi.cirera@qi.ub.es

S1. DFT Benchmark for the $[Fe(L_2^R)_3]^{2+}$ (L_2 = 3-(2-pyridyl)pyrazole) system

Method	*ΔE*	*ΔH*	*ΔS*	$T_{1/2}$
TPSSh	10.28	9.45	18.58	509
OPBE	5.67	4.84	20.21	239
OLYP	1.70	0.88	20.91	42
B3LYP	-2.87	-3.64	18.42	-198
B3LYP*	4.05	3.31	18.99	174
M06L	4.18	3.46	18.37	188

Table 1: Computed ΔE, ΔH, ΔS and $T_{1/2}$ for the $[Fe(L_2^R)_3]^{2+}$ (L_2 = 3-(2-pyridyl)pyrazole). Electronic Energies and Enthalpies in kcal·mol^{-1}. Entropies in cal·K^{-1}·mol^{-1} and all temperatures in K.

S2. Experimental values for different $[Fe_2(L_1)_3]^{4+}$ (L_1 = 1,3-bis(3-(pyridine-2-yl)-1H-pyrazol-5-yl)benzene) reported systems

System	$T_{1/2}$ *(K)*		*Refcode*	*Ref.*
	Magnetic susceptibility	Calorimetry studies		
$Cl@[Fe_2(L_1)_3]Cl(PF_6)_2\cdot 5.7CH_3OH$	305	302.1(3)	INUGIJ	1
$Br@[Fe_2(L_1)_3]Br(PF_6)_2\cdot 4CH_3OH$	265	258.2(3)	INUJOS	1
$Cl@[Fe_2(L_1)_3]Cl(PF_6)_2\cdot 3CH_3OH\cdot H_2O$	160, 265	185.0(3), 258.9(3)	INUPEO	1
$Br@[Fe_2(L_1)_3]Br(PF_6)_2\cdot CH_3OH\cdot H_2O$	≈ 200 gradual	≈ 200 gradual	INUFII	1
$Cl@[Fe_2(L_1)_3](I_3)_3\cdot 3Et_2O$	–	–	INUGAB	1
$Br@[Fe_2(L_1)_3](I_3)_3\cdot 3Et_2O$	–	–	INUGEF	1

1. M. Darawsheh, L. A. Barrios, O. Roubeau, S. J. Teat, G. Aromí, *Chem. Eur. J.*, **2016**, *22*, 8635.

S3. Computation of the transition temperatures

The goal of the code is to model the transition curve for a dinuclear SCO system. To do so, we used a variant of the Slichter and Drickamer's model for a dinuclear system. In this approach the Gibbs Free Energy can be computed as:

$$G = x \cdot G_{SS} + y \cdot G_{SQ} + z \cdot G_{QQ} + \Gamma(x,y,z) - TS_{mix}$$

Where x, y and z are the molar fractions of the low-spin/low-spin system (singlet-singlet or SS), low-spin/high-spin system (singlet-quintuplet or SQ) and high-spin/high-spin system (quintuplet-quintuplet or QQ), respectively. G_{SS}, G_{SQ} and G_{QQ} are their Gibbs free energy on the pure phases. Gamma is a function that accounts for the intermolecular interactions between cells, which can be defined as:

$$\Gamma(x,y,z) = \gamma(xy + \alpha yz + \beta zx)$$

In the Slichter and Drickamer model, it can be assumed that the interaction is just between a metal in the high spin state and another metal in the low spin state. Therefore the interaction between SS-SQ is equal to SQ-QQ and twice as SS-QQ. With that assumption, $\alpha = 1$ and $\beta = 2$.
S_{mix} is defined as the mixing entropy, and takes into account that the system is not in a pure phase, but in a mixture. This mixing entropy can be defined as:

$$S_{mix} = -k\left(N_A \cdot \ln\left(N_A\right) + N_A \cdot x \cdot ln\left(N_A \cdot x\right) + N_A \cdot y \cdot ln\left(N_A \cdot y\right) + N_A \cdot z \cdot ln\left(N_A \cdot z\right)\right) = -R(x \cdot z \cdot ln(z))$$

Where k is the Boltzmann constant, N_A is the Avogadro number and R the ideal gas constant. With all this and assuming G_{SS}=0, we can obtain the definition of Gibbs Energy used to model these systems (equation 1 in the paper) as:

$$\Delta G = y\left(\Delta H_1 - T\Delta S_1\right) + z(\Delta H - T\Delta S) + \gamma(xy + yz + 2zx) + RT(x\ln(x) + y\ln(y) + z\ln(z)) \quad [1]$$

Where $^{\Delta}H_1$ and $^{\Delta}S_1$ are the enthalpy and entropy difference from SS to SQ and $^{\Delta}H$ and $^{\Delta}S$ are the enthalpy and entropy difference from SS to QQ.

The equilibrium conditions of this system are:

$$\begin{cases} x + y + z = 1 \\ \left(\frac{\partial \Delta G(x,y)}{\partial x}\right)_T = 0 \\ \left(\frac{\partial \Delta G(x,y)}{\partial y}\right)_T = 0 \end{cases}$$

Since the problem has no analytical solution, the equilibrium conditions have been solved at various temperatures, obtaining for each one the x,y and z values that satisfy the equilibrium conditions. With that, x=f(T), y=f(T) and z=f(T) can be obtained. When using

the code, one just needs to specify the $^{\Delta S_1}$, ΔS, ΔH, γ and W. W is a different way to introduce $^{\Delta H_1}$ since it is defined as: $W = \Delta H_1 - \Delta H/2$.

The temperature at which x(T) = y(T), is the transition temperature for the first step transition (SS-SQ), and when y(T)=z(T), we have the transition temperature for the second step transition (SQ-QQ). Finally, when x(T)=z(T), we obtain the transition temperature for the SS-QQ transition.

To obtain the effective magnetic moment at each temperature, we just need to multiply $4.9\mu_B$, which is the spin-only value for and Fe^{2+}ion, by the y value and add it two times $4.9\mu_B$ multiplied by the z molar fraction (since QQ have two iron ions in high-spin state whereas QS just have one). So, μ_{eff} can be estimated with the expression:

$$\mu_{eff}(T) = 4.9 \cdot (y(T) + 2 \cdot z(T))$$

If its derivative with respect of temperature has two maximum, we assume a two-step transition. However, if it has only one maximum, the transition is classified as a one-step transition.

It is important to remark that this model does not account for incompleteness of the transition both at very low and high temperatures, where the system is mainly in low spin and high spin state, respectively. However, it reproduces the magnetic behaviour of the studied systems quite accurately.

S4. Effect of the functionalization on the $[Fe(L_2^R)_3]^{2+}$ (L_2 = 3-(2-pyridyl)pyrazole)) system.

Functionalization of the pyridine ring

$[Fe(L_2^{R1})_3]^{2+}$	ΔH	ΔS	$T_{1/2}$
-F	8.31	18.49	450
-H	9.45	18.577	509
$-OCH_3$	8.45	18.07	467
-Cl	8.84	18.66	474
$-CH_3$	9.45	18.92	500

Table 1: Computed ΔH, ΔS and $T_{1/2}$ for the $[Fe(L_2^R)_3]^{2+}$ (L_2 = 3-(2-pyridyl)pyrazole, R_1 = -H, $-CH_3$, $-OCH_3$, -F and -Cl). Enthalpies in kcal·mol^{-1}, entropies in cal·K^{-1}·mol^{-1} and temperatures in K.

Functionalization of the pyrazole ring

$[Fe(L_2^{R2})_3]^{2+}$	ΔH	ΔS	$T_{1/2}$
-F	8.47	17.76	477
-H	9.45	18.577	509
$-OCH_3$	10.00	17.68	566
-Cl	10.19	20.06	508
$-CH_3$	10.99	18.06	609

Table 2: Computed ΔH, ΔS and $T_{1/2}$ for the $[Fe(L_2^R)_3]^{2+}$ (L_2 = 3-(2-pyridyl)pyrazole, R_2 = -H, $-CH_3$, $-OCH_3$, -F and -Cl). Enthalpies in kcal·mol^{-1}, entropies in cal·K^{-1}·mol^{-1} and temperatures in K.

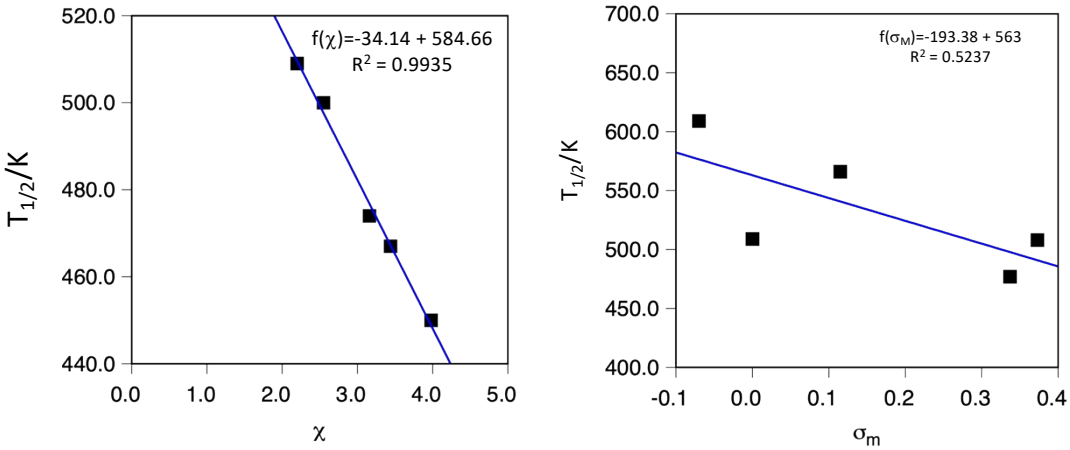

Left, correlation between the computed $T_{1/2}$ and the electronegativity of the atom in the para position for the pyridyl ring functionalization. Right, correlation between the σ_m Hammett constant and the computed $T_{1/2}$ for the pyrazole ring functionalization.

S5. Transition temperature dependence on guest radius

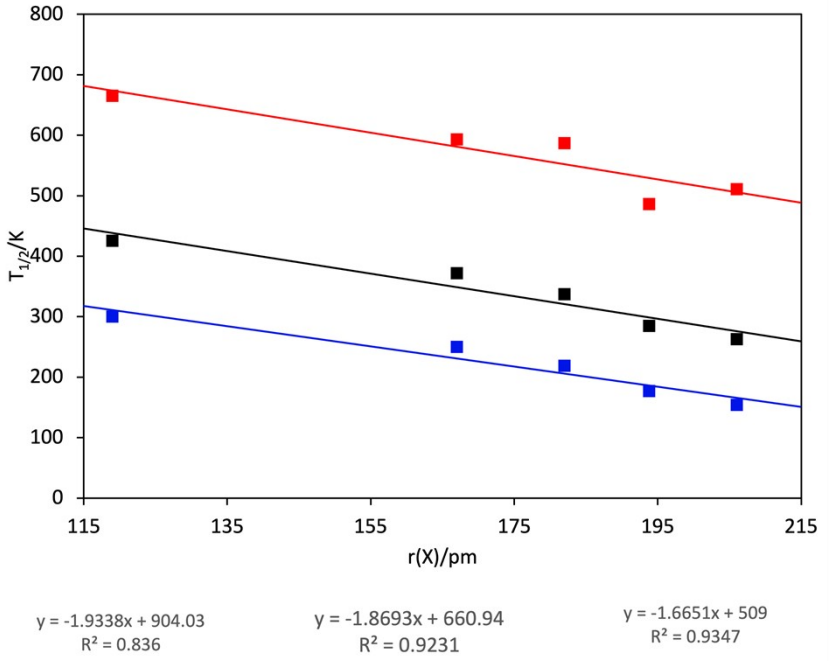

Transition temperature dependence on the guest ionic radius.[1] Red: R = -CH_3 (R^2 = 0.84), black: R = -H (R^2 = 0.92) and blue: R = -F (R^2 = 0.93).

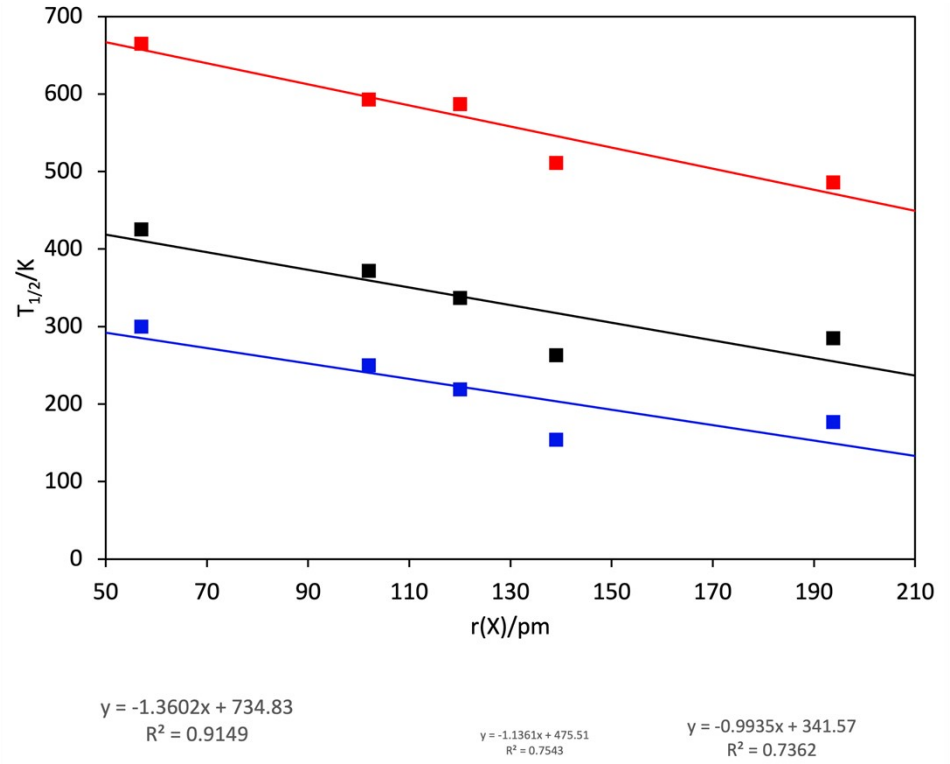

Transition temperature dependence on the guest covalent radius.[2] Red: R = -CH_3 (R^2 = 0.91), black: R = -H (R^2 = 0.75) and blue: R = -F (R^2 = 0.74).

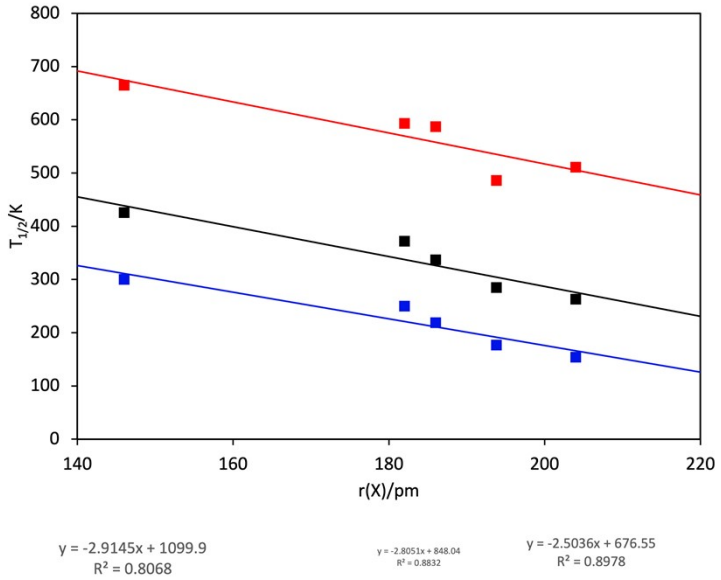

Transition temperature dependence on the guest Van der Waals radius.[3] Red: R = -CH_3 (R^2 = 0.81), black: R = -H (R^2 = 0.88) and blue: R = -F (R^2 = 0.90).

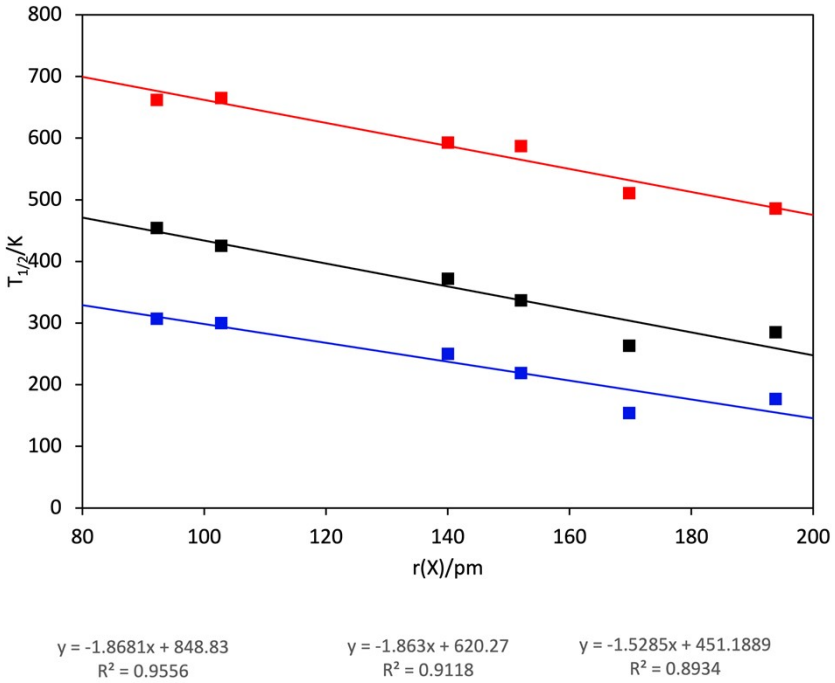

Transition temperature dependence on the DFT computed guest radius.[4] Red: R = -CH_3 (R^2 = 0.96), black: R = -H (R^2 = 0.91) and blue: R = -F (R^2 = 0.89).

1. R. D. Shannon, C. T. Prewitt, *Acta Cryst. B*, **1969**, *25*, 925; R. D. Shannon, *Acta Cryst. A*, **1976**, *32*, 751.
2. B. Cordero, V. Gómez, A. E. Platero-Prats, M. Revés, J. Echeverría, E. Cremades, F. Barragán, S. Alvarez, *Dalton Trans.,* **2008**, 2832.
3. S. Alvarez, *Dalton Trans*., **2013**, *42*, 817.
4. Jian-Biao Liu, W. H. Eugen Schwarz, Jun Li, *Chem. Eur. J.*, **2013**, *19*, 14758; M. A. Blanco, A. Costales, A. Martín-Pendás, V. Luaña, *Phys. Rev. B*, **2000**, *62*, 12028.

S6. Cartesian coordinates and output calculations additional data

A data set collection of computational results is available in the ioChem-BD repository[1] and can be accessed via https://iochem-bd.bsc.es/browse/handle/100/322091

1. M. Álvarez-Moreno, C. de Graaf, N. Lopez, F. Maseras, J. M. Poblet, C. Bo, *J. Chem. Inf. Model*. **2015**, 55, 95.

S7. Schematic d-based Molecular Orbital Diagrams for the $[Fe_2(L_1^R)_3]^{4+}$ and $([Fe_2(L_1^R)_3@F)^{3+}$ systems

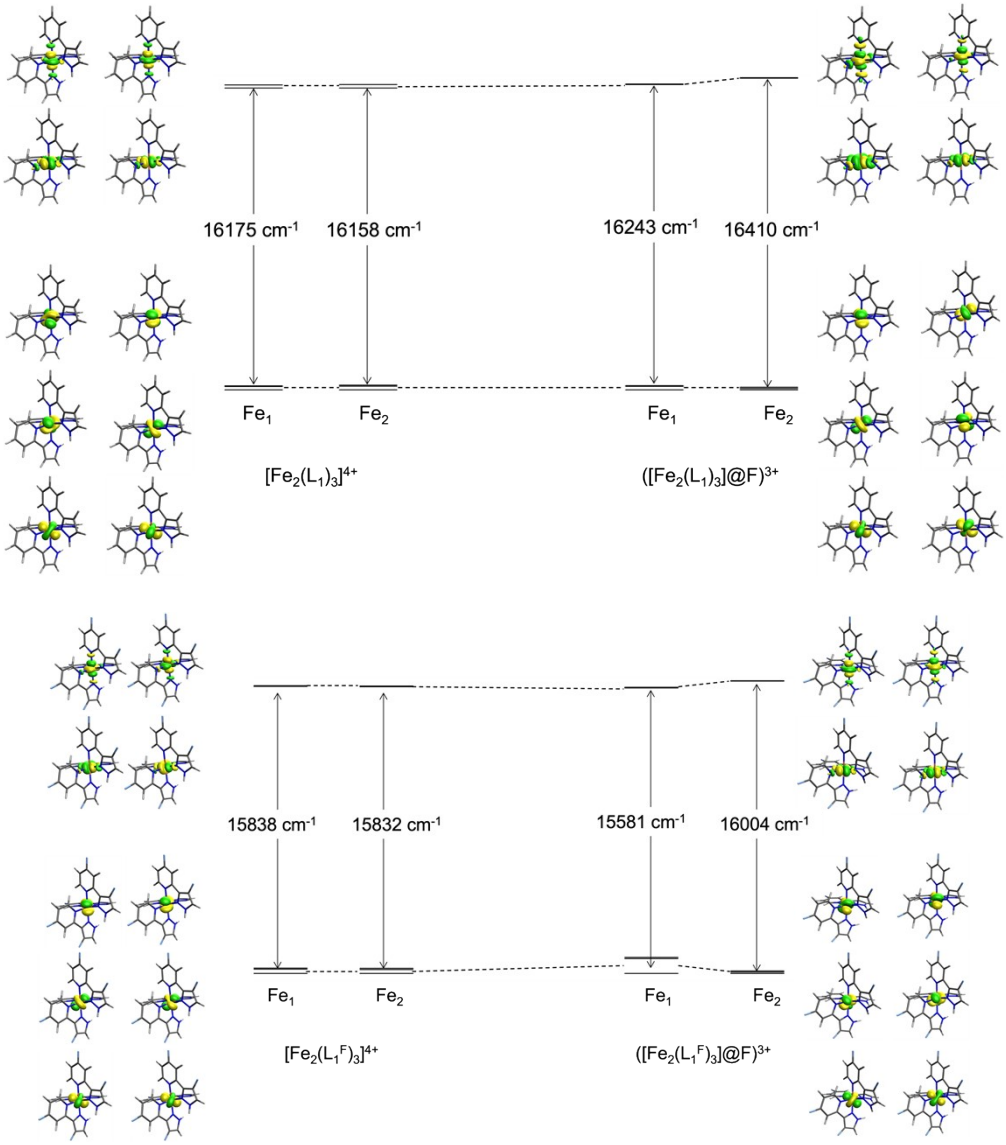

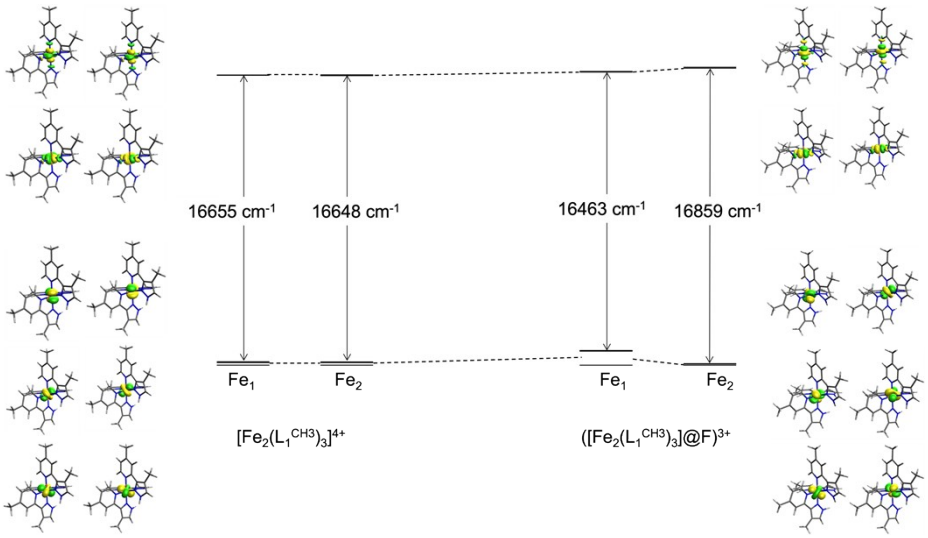
16655 cm-1
16648 cm-1
16463 cm-1
16859 cm-1
Fe1
Fe2
Fe1
Fe2
[Fe2(L1CH3)3]4+
([Fe2(L1CH3)3]@F)3+

S8. NEVPT2/AILFT analysis of the d-based molecular orbitals

d-MOs splitting for the $[Fe_2(L_1^R)_3]^{4+}$ (R = H, F or CH_3). All energies in cm^{-1}.

R = H		R = F		R = CH_3	
Fe_1	Fe_2	Fe_1	Fe_2	Fe_1	Fe_2
16175	16158	15838	15832	16655	16648

d-MOs splitting for the $[Fe_2(L_1^R)_3]@F^{3+}$ (R = H, F or CH_3). Fe_1 is the closest to the F^- anion. All energies in cm^{-1}.

R = H		R = F		R = CH_3	
Fe_1	Fe_2	Fe_1	Fe_2	Fe_1	Fe_2
16243	16410	15881	16004	16463	16859

CShM(OC-6) for the Fe_1/Fe_2 and F^- distance to each metal center. Distances in Å.

	R = H		R = F		R = CH_3	
	Fe_1	Fe_2	Fe_1	Fe_2	Fe_1	Fe_2
CShM(OC-6)-F	1.15	0.90	1.12	0.87	1.10	0.93
r(Fe-F)	3.906	5.957	3.882	6.002	3.862	5.946
CShM(OC-6)-Br	0.890	0.891	0.866	0.867	0.916	0.916
r(Fe-Br)	4.759	4.760	4.766	4.767	4.766	4.767

S9. Effect of γ value on the shape of the spin-transition for the $([Fe_2(L_1^F)_3]@Cl)^{3+}$ system

Impact of γ value on rate of change of the spin-state populations and the shape of the spin-transition for the $([Fe_2(L_1^F)_3]@Cl)^{3+}$ system. For that system, ρ = -0.10, which leads to a single step transition if γ = 0 and a two-step transition if γ = 3740 J/mol (red line). Colour code for ω_i : i = [LS-LS] (blue), [HS-LS] (green) and [HS-HS] (red) populations. Notice that increasing γ does not change the crossing point temperature between spin-state populations.

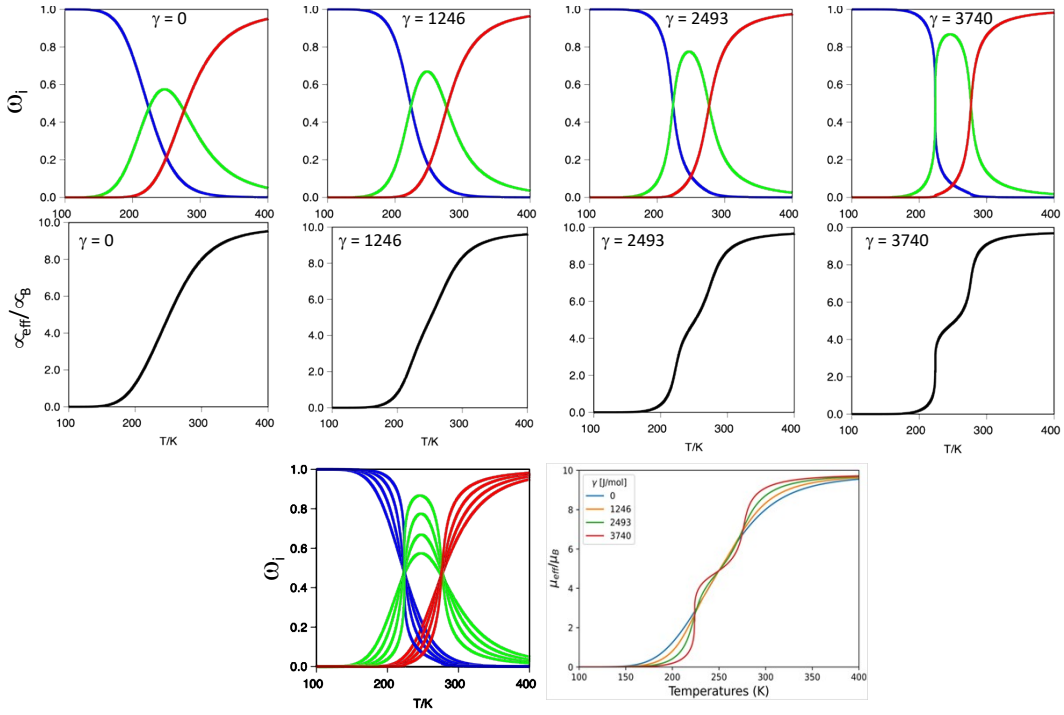

S10: Spin state populations and magnetic moment for the $([Fe_2(L_1^{CH3})_3]@F)^{3+}$ system

Left, Spin state populations (ω_i) for the $([Fe_2(L_1^{CH3})_3]@F)^{3+}$ system, with $\rho = -0.14$ and $\gamma = 0$ J/mol. i = [LS-LS] (blue), [HS-LS] (green) and [HS-HS] (red) populations. Right, estimation of the magnetic moment computed form the corresponding spin-state populations.

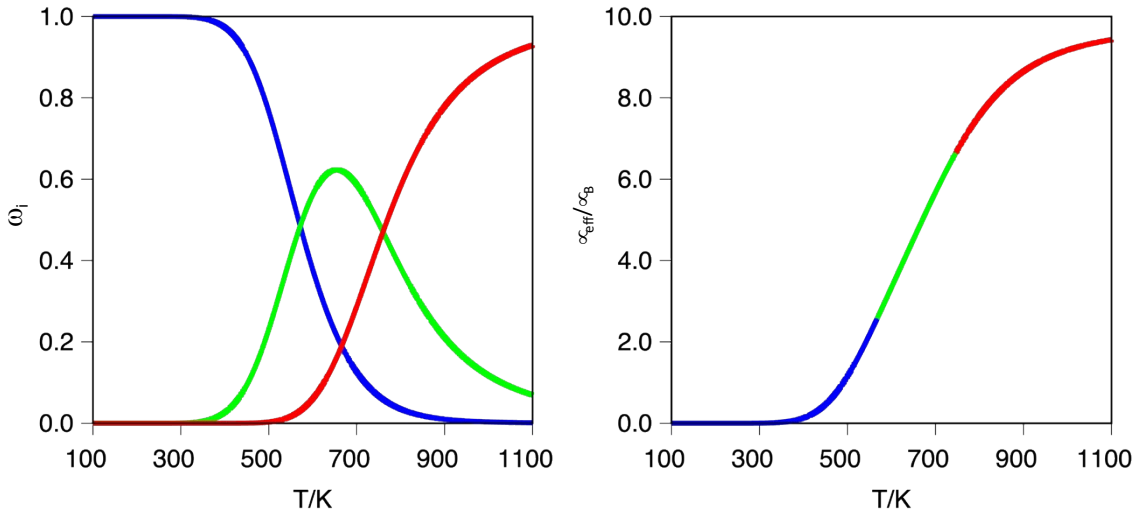

S11. Effect of the guest atom on the Fe-N bond lengths.

Correlation between the Fe-N average bond length and the guest size for the $([Fe_2(L_1^{R})_3]@X])^{3+}$ (X = H^-, F^-, Cl^-, Br^- and I^-, R = -H, -F or $-CH_3$) systems.

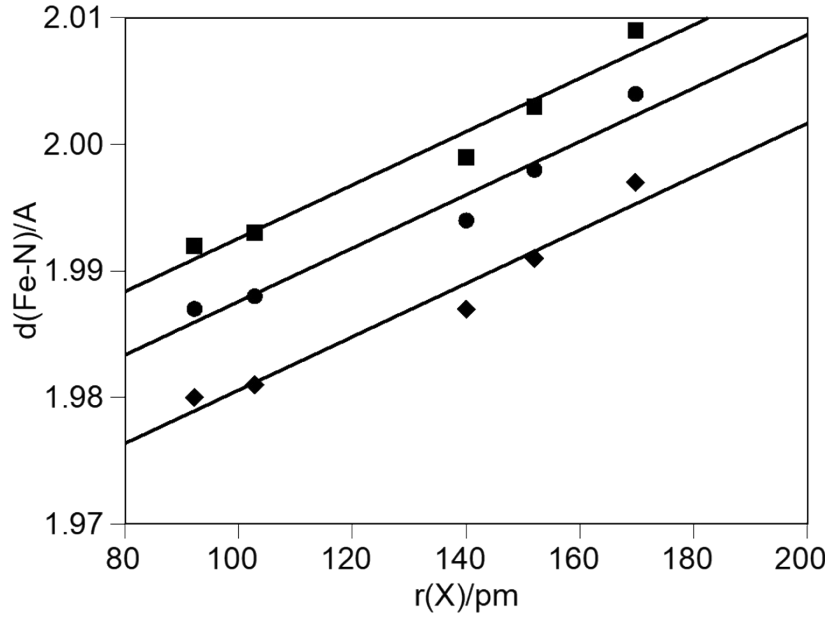

$([Fe_2(L_1^{R})_3]@X])^{3+}$ where R = -F (squares), -H (circles) and $-CH_3$ (diamonds)

S12 Analysis of the anion $[BF_4]^-$ as guest

The $[BF_4]^-$ anion has a tetrahedral shape, which makes difficult to compare it with the spherical ones (X = H^-, F^-, Cl^-, Br^- and I^-). However, one can estimate its radii by surveying the B-N bond length in the $[BF_4]^-$ structurally characterized systems as they appear in the Cambridge Structural Database.

This analysis has been done on 10272 fragments, which leads to an average bond length of 137 +/- 3 pm (99% confidence interval). This is, however, the distance between the boron and F. One must add half the covalent radii of the fluoreine atom to get an actual estimation of the radii. Using the F covalent radii (57 pm) leads to an estimated radii for the $[BF_4]^-$ of 193.8 pm.

Using this value, one can add the computed $T_{1/2}$ to the correlation plots, which essentially, remains unaltered.

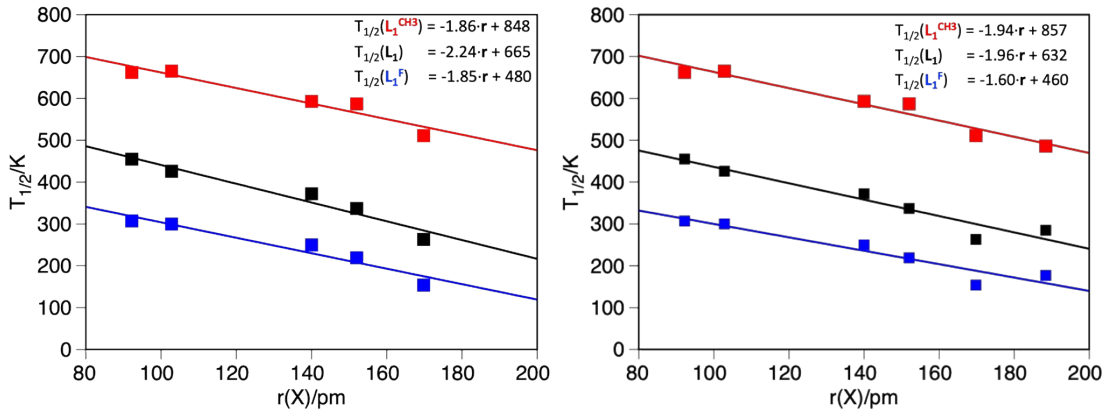

Figure S12.1: Left, correlation between $T_{1/2}$ and the guest size without $[BF_4]^-$. Right, the same correlation including the $[BF_4]^-$ anion.

The shape of $[BF_4]^-$ is unique, and so it is its spatial arrangement within the cavity. That is the reason that makes the analogy with spherical guest quite difficult. A close inspection of the spatial arrangement of the anion inside the cavity shows that one of the F groups is pointing towards one of the Fe^{II} metal centers, much like the F^-, does, but cannot get as close as fluorine does because of the remaining part of the anion. Also, the B atom is not in the central part of the molecule, which means that one vertex of the tetrahedron is pointing towards on the Fe metal centers (see figure below). This anisotropic arrangement can be, indeed, the source of its different behavior towards the computed $T_{1/2}$.

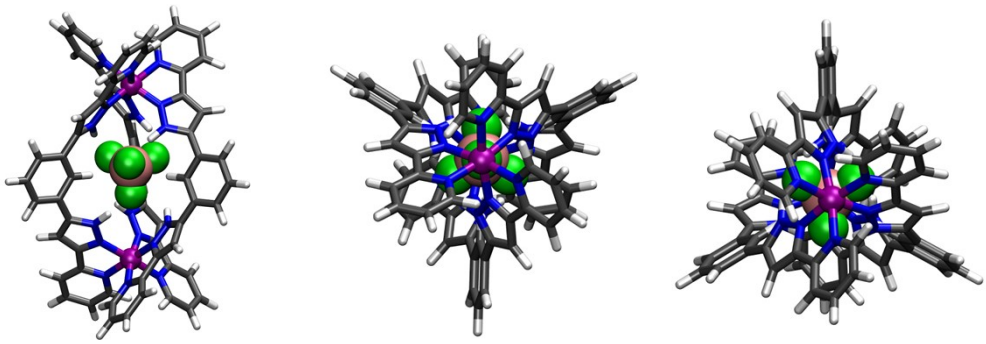

Figure S12.2: Front, back and forth view of the $([Fe_2(L_1)_3]@BF_4)^{3+}$ system, showing the unique orientation of the anion inside the cavity.